Centrality Definition Using Mid-Rapidity E_T distributions from p+Be to Au+Au at AGS Energies

M. J. TANNENBAUM
for The E802 Collaboration
Brookhaven National Laboratory
Upton, NY 11973-5000 USA

Measurements by the E802 Collaboration of the A-dependence and pseudorapidity interval ($\delta\eta$) dependence of mid-rapidity E_T distributions in a half-azimuth electromagnetic calorimeter are presented for p+Be, p+Au, O+Cu, Si+Au and Au+Au collisions at the BNL-AGS. The issues addressed are 1) whether the shapes of the upper edges of the E_T distributions vary with $\delta\eta$ similarly to the variation in shapes of mid-rapidity charged particle distributions and 2) how small a $\delta\eta$ interval would still give a meaningful characterization of the 'nuclear geometry' of a reaction.

The shapes of E_T distributions as characterized by the p parameter of a Gamma Distribution vary are observed to systematically with the size of the $\delta\eta$ interval. However, in contrast to the situation for Multiplicity Distributions where the shape as characterized by the NBD parameter $1/k(\delta\eta)$ can be related to the 2-particle short-range correlation length, there is at present no theoretical framework to relate the systematic variation in the shapes of E_T distributions to other physical quantities. On the other hand, the Wounded Projectile Nucleon model works remarkably well to relate all the measured spectral shapes of Electromagnetic E_T distributions from p+Be, p+Au, to O+Cu, to Si+Au to Au+Au at AGS energies for pseudorapidity intervals $\delta\eta$ in the range $0.2 \leq \delta\eta \leq 1.25$ around mid-rapidity. Hence, it is clear that midrapidity E_T distributions in limited regions of $\delta\eta$ provide an excellent characterization of the 'nuclear geometry' of RHI collisions, from which important information about the dynamics can be inferred. For instance, the variation of such quantities as impact parameter, number of participants, etc, can be estimated as a function of the measured E_T, which may be relevant to discussions of 'sharp changes' of measured physical quantities as a function of measured E_T in electromagnetic calorimeters.

Quark Matter 99, Torino, Italy, May 1999

E802/E859/E866 Midrapidity E_T Measurements In PbGlass Electromagnetic Calorimeter

♡ $E_T \equiv \sum_{\text{photons}} E_\gamma \sin\theta + \sum_{\text{charged, } \beta \geq 0.8} (0.45 \text{ GeV}) \times \sin\theta$

♡ The measure is precise but not accurate.

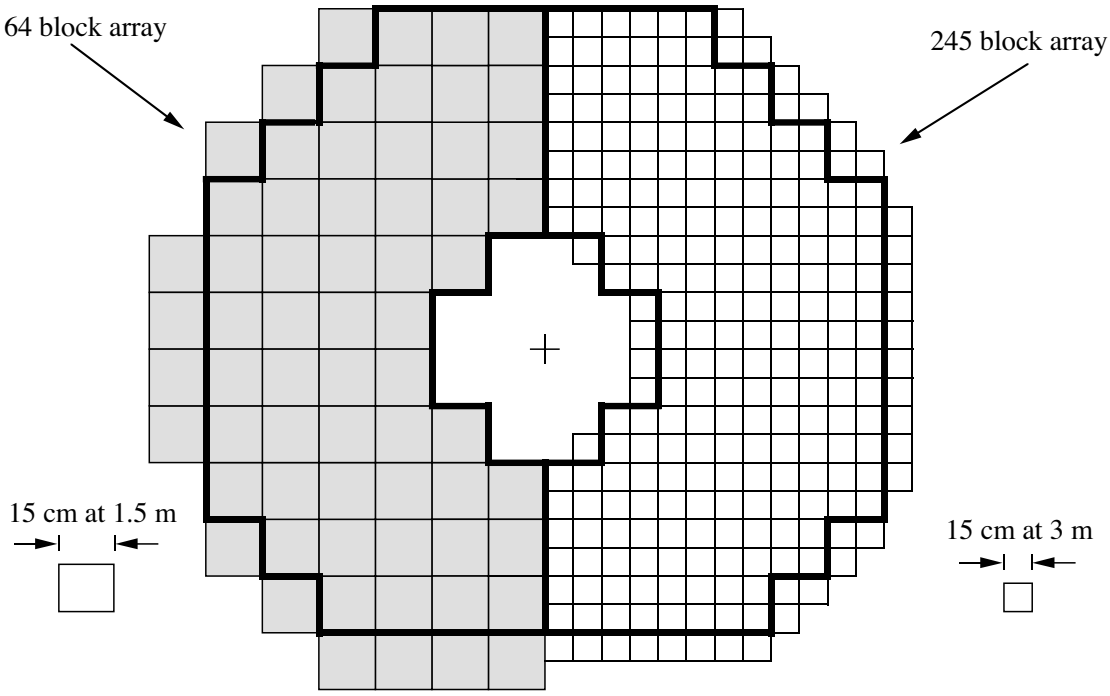

Fig. 1

Figure 1: E802/E859/E866 PbGl Detector. The $\delta\eta$ dependence is made using the more highly segmented right side of the calorimeter.

E_T and Multiplicity Distributions

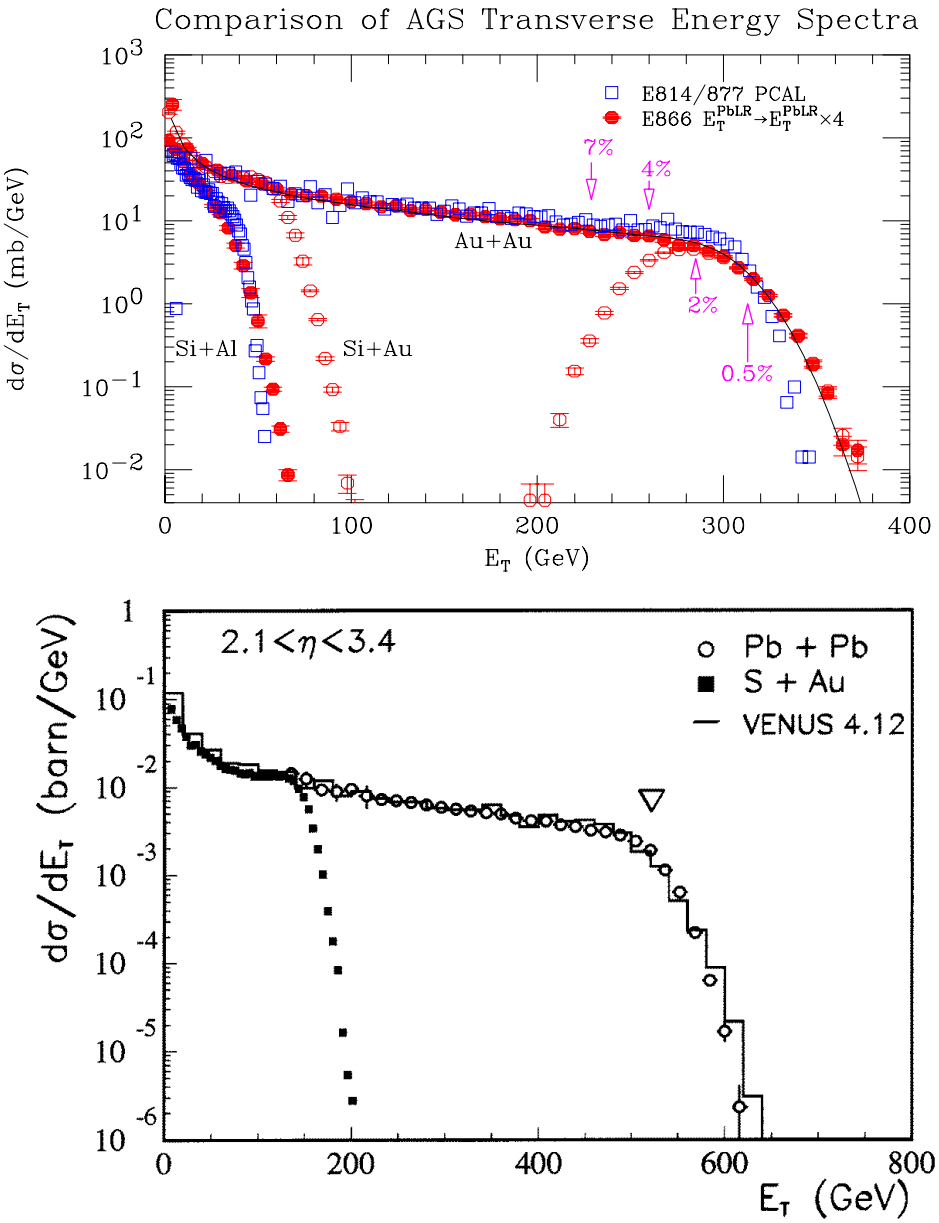

Figure 2: Top(t): AGS measurements—E814/E877 E_T spectra in a full-azimuth hadron calorimeter compared to E802/E866 full azimuth E_T spectra in an EM calorimeter covering a smaller pseudorapidity interval. E802/E866 data include a central Au+Au spectrum defined by the 4 %-ile of the distribution in a Zero Degree Calorimeter (ZCAL). The solid line on the E802/E866 Au+Au data is an empirical calculation (see text). Bottom(b): CERN measurement—NA49 mid-rapidity E_T spectrum in a full-azimuth hadron calorimeter.

'Centrality' and percentiles of E_T distributions

♡ At the AGS E802/E866 and E814/E877 use E_T in an Electromagnetic or hadronic calorimeter to define 'centrality', typically by a certain upper percentile of the distribution.

♡ The less constrained distributions measured by E802/E866 in an EM calorimeter covering $1.3 \leq \eta \leq 2.4$ (and scaled by a factor of 4 in E_T for visual effect) fluctuate more than the more constrained distributions measured by E814/E877 in a hadron calorimeter covering $0.83 \leq \eta \leq 4.7$.

♡ **But** for the most part the distributions are very similar in shape, and therefore in Centrality Definition.

♡ The E_T spectra measured by NA49 in a mid-rapidity hadron calorimeter at CERN show the more rounded upper edges, similar to the AGS mid-rapidity distributions.

♡ The E_T emission in Au+Au (Pb+Pb) relative to Si+Au can be simply read from Fig. 2 and is clearly $\sim$ 20% larger at AGS energies compared to CERN. This is likely a reflection of the 'stopping' at AGS energies which depresses the energy emission from successive collisions in asymmetric (Si+Au) reactions compared to the symmetric case (Si+Al).

INTERMITTENCY isn't CHAOS

♡ It is well known, by now, that the shapes of multiplicity distributions for central collisions of relativistic heavy ions change with the size of the region of phase space in which they are measured—even for relatively 'small' changes of pseudorapidity interval in the range $0.1 \leq \delta\eta \leq 1.0$.

♡ This phenomenon, originally developed in terms of the Normalized Factorial Moments of the multiplicity distributions and dubbed 'intermittency', has been explained by the dramatic reduction of the two-particle short-range rapidity correlation length ξ in central RHI collisions to a value, $\xi \sim 0.2$, which is much shorter than the value $\xi \sim 1 - 3$ in nucleon-nucleon collisions.

♡ The standard hadron short-range correlations vanish, as predicted, with increasing centrality—since the chance of getting two hadrons from the same elementary collision decreases like the number of collisions—while only the quantum-mechanical Bose-Einstein correlations remain.

♡ The fact that the rapidity correlation length from B-E interference was so short, $\xi_y = 0.19 \pm 0.03$, was not generally appreciated until demonstrated recently by E802 [PRC **56**, 1544 (1997)] in agreement with the multiplicity shape analysis.

♡ One assumes that the same effect, the variation in shape as a function of the pseudorapidity interval, $\delta\eta$ must occur with E_T distributions, but would likely be different in detail in calorimeters.

E802 O+Cu Central Multiplicity Distributions vs. $\delta\eta$

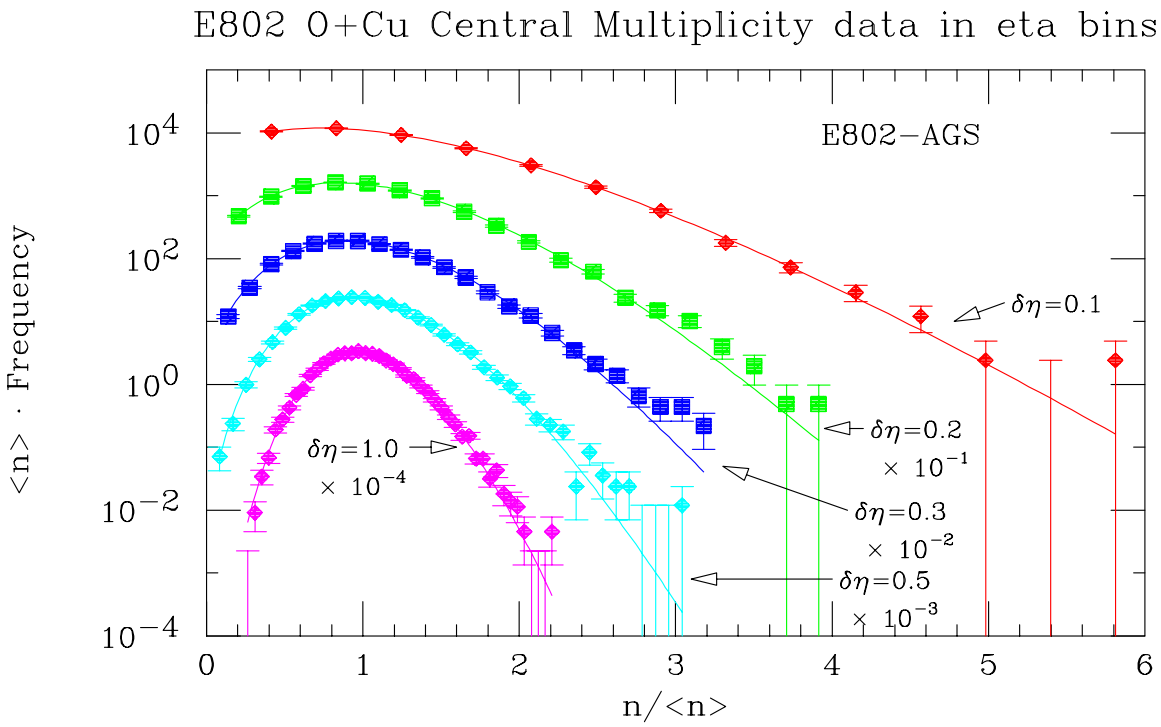

Figure 3: Multiplicity distributions measured in ^{16}O+Cu central collisions as a function of the interval $\delta\eta$ (indicated), scaled by $< n >$ on the interval, for the case when all 16 incident nucleons have interacted as determined by the ZCAL.

♡ The shape of the charged multiplicity distribution varies from nearly exponential for $\delta\eta = 0.1$ to nearly gaussian for $\delta\eta = 1.0$.

♡ The shape of multiplicity distributions, as parameterized by Normalized Factorial Cumulants $K_q(\delta\eta)$ or by the NBD parameter $1/k(= K_2)$, is determined by 2-particle correlations in an elegant theoretical framework.

Mid-Rapidity E_T distributions

♡ As E_T measurements in limited solid angles have recently become quite popular to characterize the 'centrality' of RHI collisions, systematic investigations were made of the A dependence of such mid-rapidity E_T distributions as a function of the $\delta\eta$ interval.

♡ An important issue is that models have proved useful in the understanding of the detailed shape of E_T distributions in B+A collisions as a sum of independent p+A collisions weighted according to the 'geometric' probability of the number of total or projectile participants in the reaction. If the 'shape' of E_T distributions were controlled by a correlation length and strength which changed with the number of participants **differently** from the effect of random combinations, then these simple models would make no sense, and, in particular, would fail to reproduce the shapes of the upper edges of the spectra.

OXYGEN + Au at 14.5 GeV/c per Nucleon

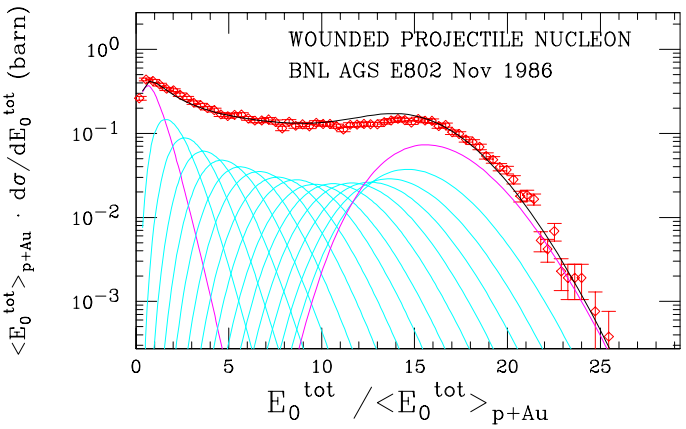

OXYGEN + Cu AT 14.5 GeV/c per Nucleon

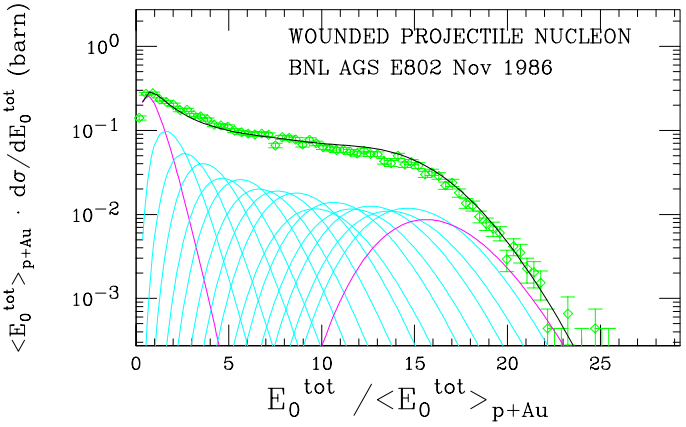

Physics or Acceptance?

♡ It is also conceivable that the saturation of the upper edges of the E802 E_T spectra at AGS energies could be an artifact of the limited angular (η) acceptance.

♡ In heavy ion collisions, the pseudorapdidity acceptance is an issue because naive models of successive collisions predict that the rapidity of the c.m. system, e.g. for a given projectile nucleon, shifts towards the target rapidity after each collision with a target nucleon—and vice-versa—such that the maximum in dn/dy and presumably $dE_T/d\eta$ moves towards the larger nucleus in an asymmetric B+A reaction. Therefore, an important issue to address is whether and how the pseudorapidity acceptance of E_T distributions affects the physical interpretion of the measurement.

♡ It is known that the projectile dependence of a reaction is emphasized by measurements in the projectile fragmentation region, while the target dependence is emphasized by measurements in the target fragmentation region—thus, mid-rapidity measurements might represent a reasonable global average.

♡ An additional issue is whether the shapes of mid-rapidity E_T distributions change with the interval, $\delta\eta$.

Mid-Rapidity E_T distributions vs $\delta\eta$

The E_T distributions (in $\Delta\phi = \pi$) were measured for successively smaller $\delta\eta$ intervals centered on $\eta|_0 \sim 1.86$: $1.25 \leq \eta \leq 2.50$ (the full η-acceptance of the calorimeter); $1.38 \leq \eta \leq 2.34$; $1.54 \leq \eta \leq 2.18$; $1.70 \leq \eta \leq 2.02$; $1.70 \leq \eta \leq 1.86$.

O+Cu Au+Au

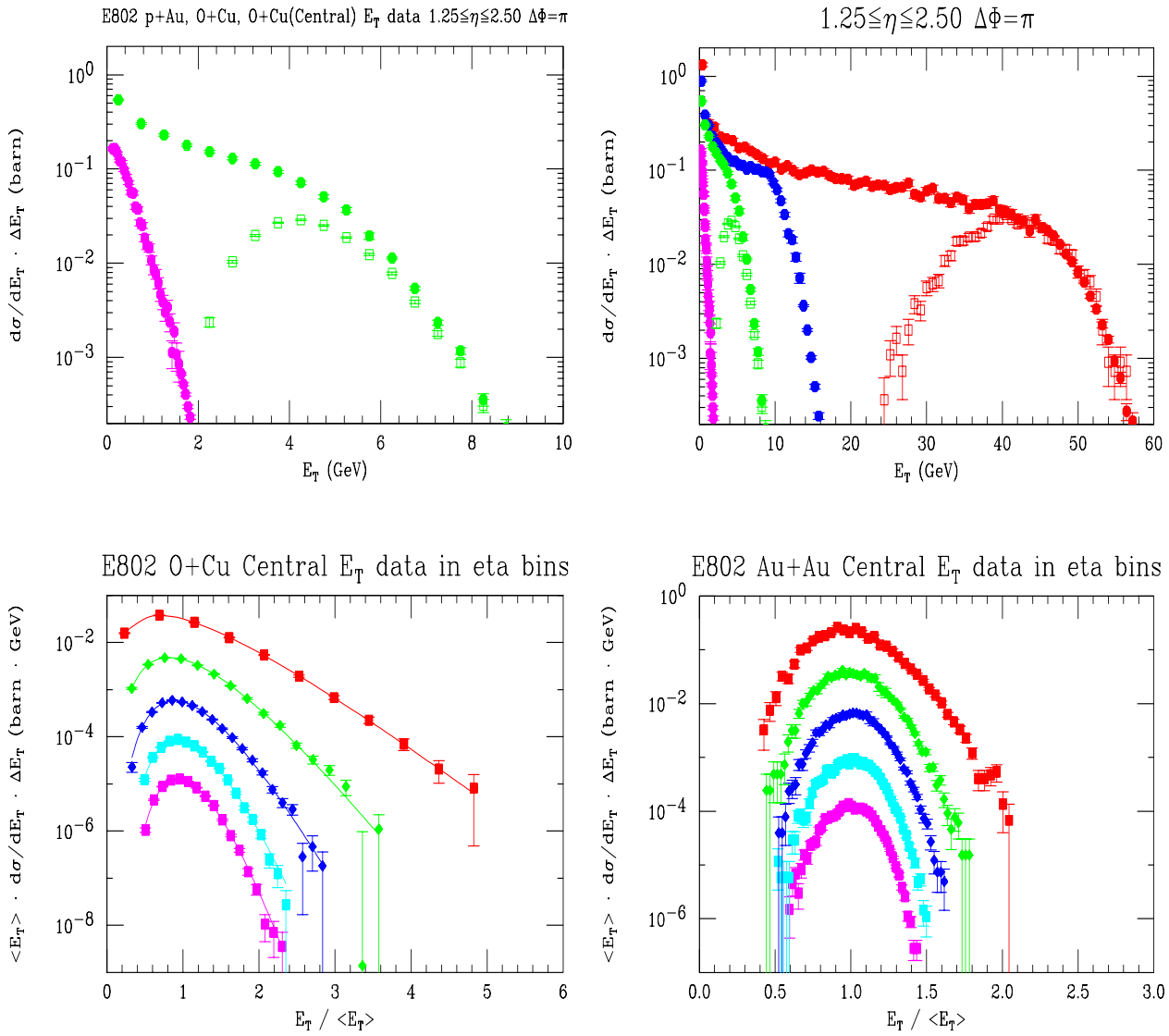

Figure 4: Top: E802 mid-rapidity E_T distributions ($\Delta\phi = \pi$) for the interval $1.25 \leq \eta \leq 2.50$. (Left) p+Au, O+Cu, O+Cu(ZCAL); (Right) previous data, plus Si+Au, Au+Au, Au+Au(ZCAL). Bottom: Central (ZCAL) E_T distributions for the five $\delta\eta$ intervals, normalized by $< E_T >$ on the interval. O+Cu (left), Au+Au (right). The curves are fits to Γ distributions.

Evidently, the shapes of the upper edges of E_T distributions change with $\delta\eta$, similarly to multiplicity.

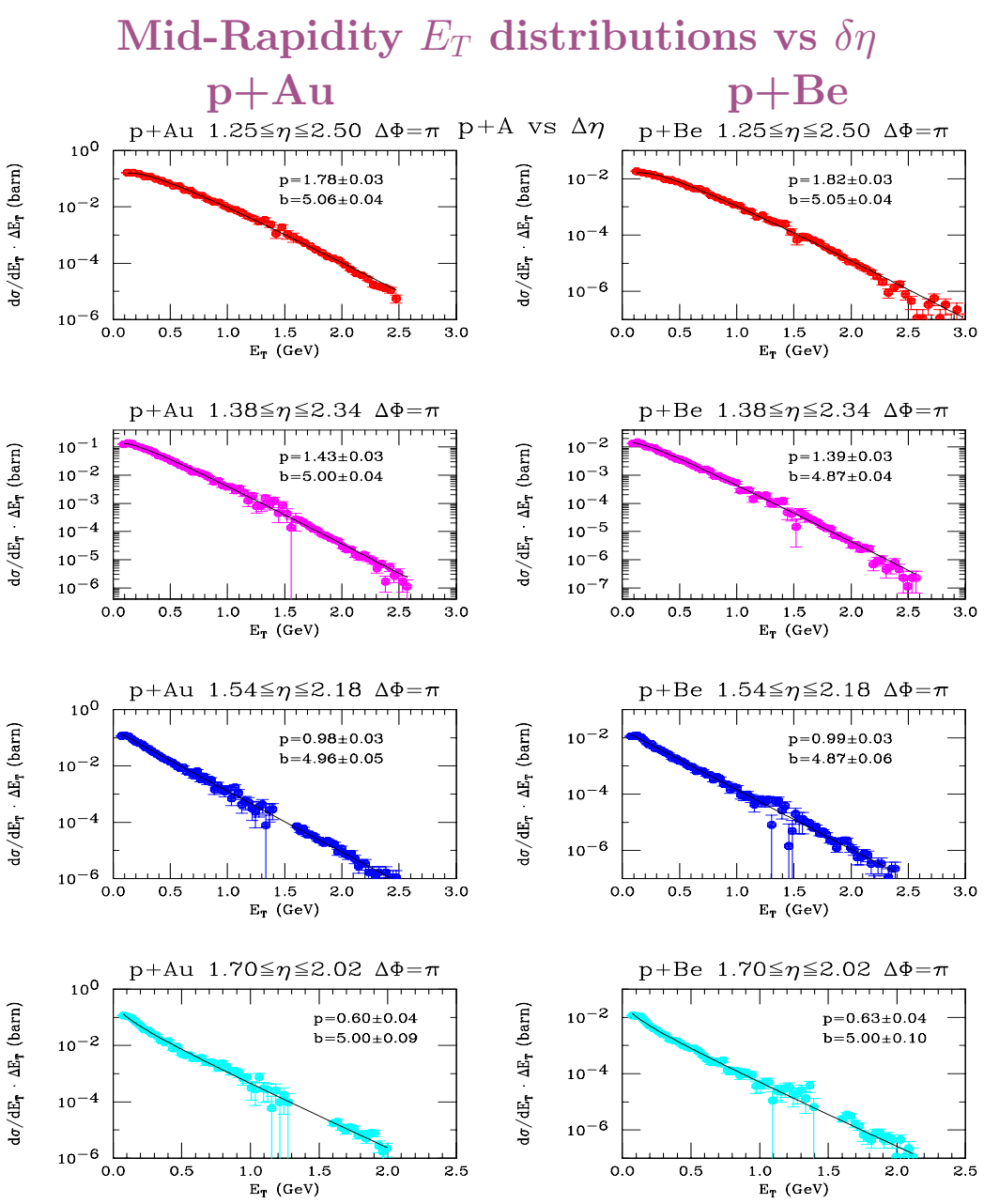

Figure 5: E_T distributions for p+Au (left) and p+Be (right) as a function of decreasing $\delta\eta$ from top to bottom. Adjacent p+Au and p+Be plots have the same $\delta\eta$.

The original E802 measurements showed that the mid-rapidity E_T spectra of p+Au, p+Cu, p+Al and p+Be all exhibit the same shape over roughly 5 decades of cross section—no obvious multiple collisions effects were evident at mid-rapidity for p+A at AGS energies. In the present measurement, as the $\delta\eta$ interval is reduced, the shapes of the E_T spectra clearly change with $\delta\eta$ for both p+Au and p+Be; but in each $\delta\eta$ interval, the shapes of the p+Au and p+Be distributions remain essentially **identical** with each other.

p parameter of Gamma Fits in B+A and $\langle E_T \rangle_{\mathrm{p+A}} = p/b$ as a function of $\delta\eta$

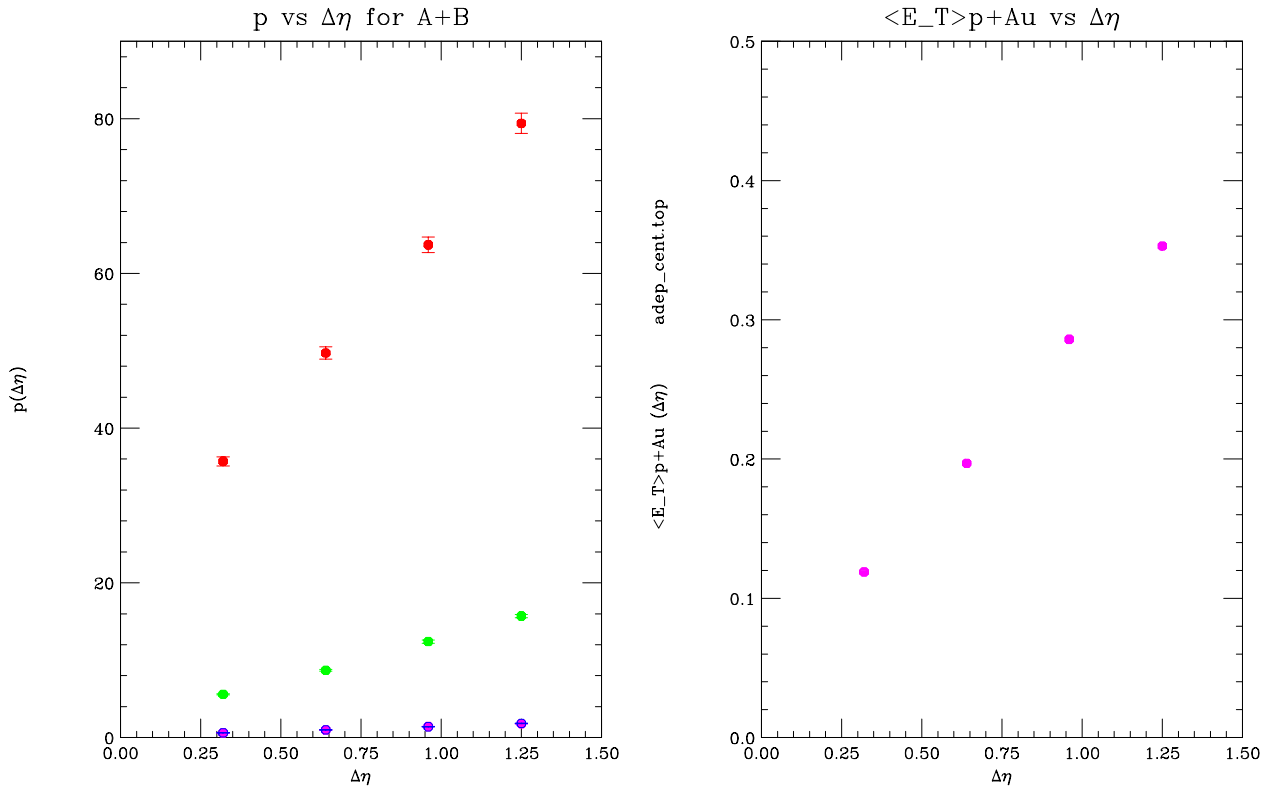

Figure 6: (left) Gamma Fit parameter p as a function of $\delta\eta$ interval for p+Be (Blue), p+Au (Magenta), O+Cu (ZCAL) (green), Au+Au (ZCAL) (red). (right) $\langle E_T \rangle_{\mathrm{p+A}}$ as a function of $\delta\eta$.

♡ Data show nice systematic behavior.

♡ No theoretical framework was found in the literature to help further interpret these results.

The Wounded Projectile Participant Model Is Preserved as a function of $\delta\eta$

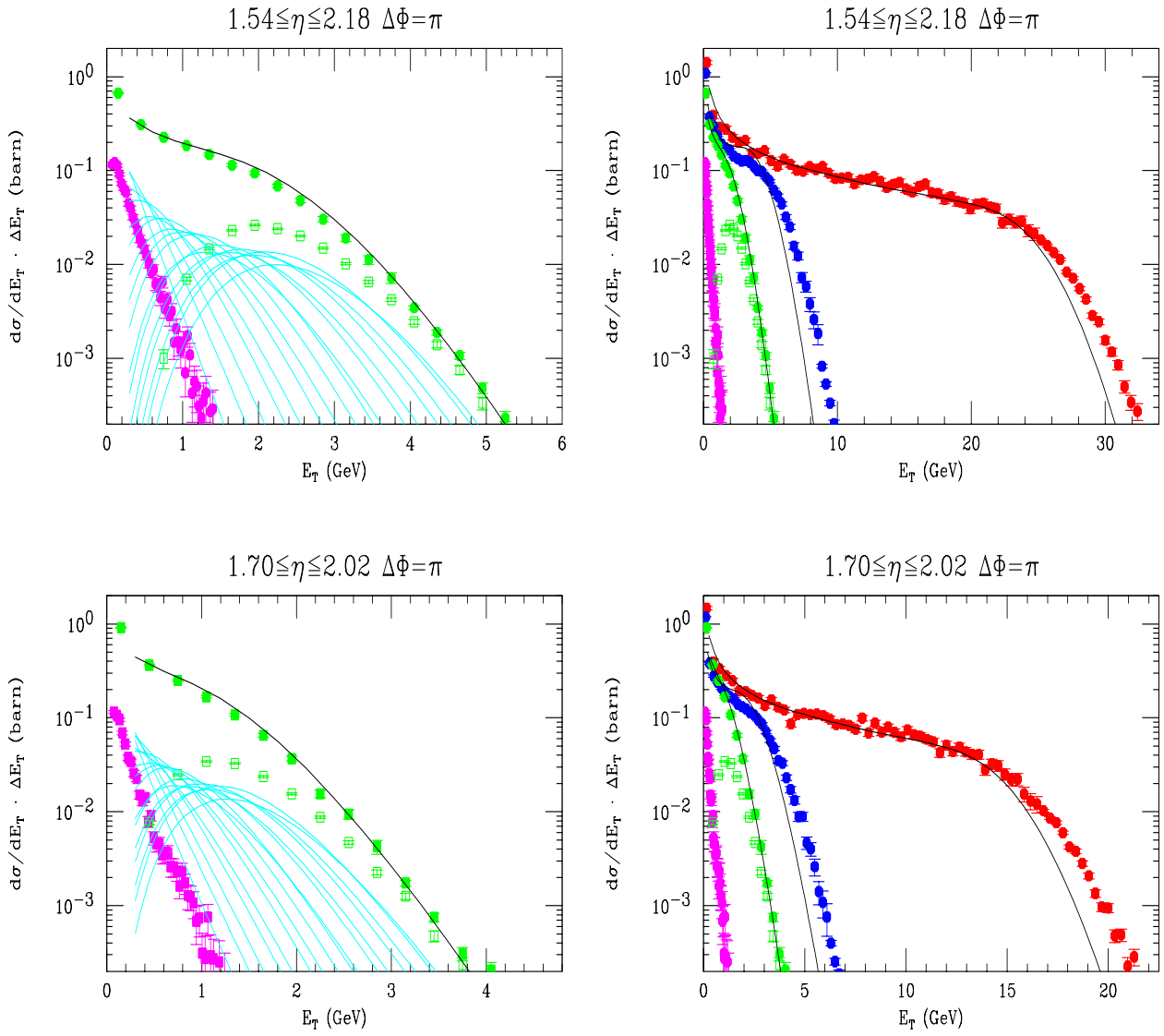

Figure 7: WPNM calculations (lines) for the two smallest $\delta\eta$ intervals for (left) O+Cu, (right) Si+Au, Au+Au. Components are shown for O+Cu. Data shown are (left) p+Au, O+Cu, O+Cu (ZCAL); (right) same data plus Si+Au, Au+Au.

As smaller and smaller $\delta\eta$ intervals are used for the E_T spectra, the probability p_0 for a p+Au reaction to produce zero signal on the interval becomes larger and larger. This effect is easily measured from the ratio of detected cross section in the $\delta\eta$ interval to the inelastic p+Au cross section (1662mb), and must be taken into account when performing the WPNM.

Distribution of Projectile Participants at a fixed E_T

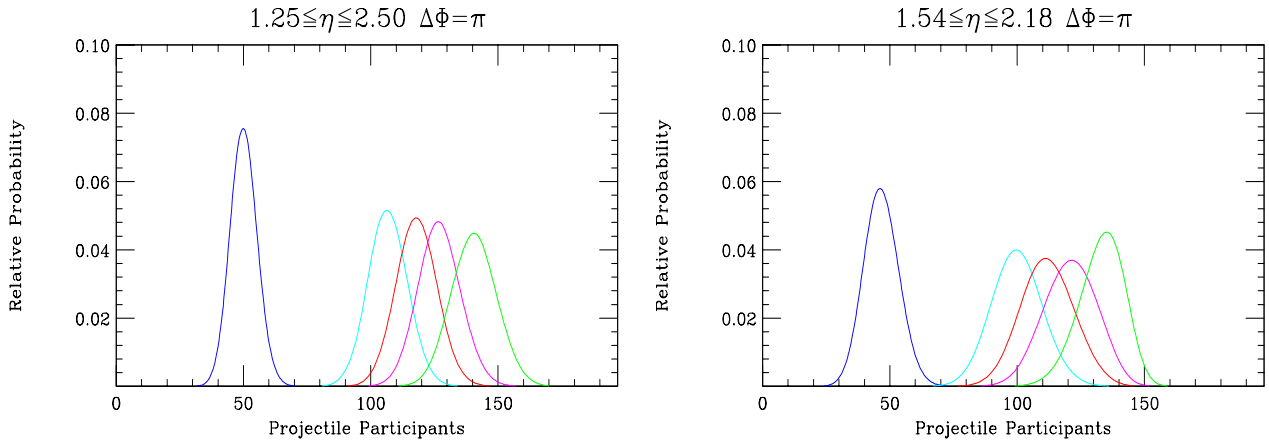

Figure 8: Distribution in Projectile Participants as a function of measured E_T ($\Delta\phi = \pi$) for two $\delta\eta$ intervals : (left) $1.25 \leq \delta\eta \leq 2.50$, (right) $1.54 \leq \delta\eta \leq 2.18$. The distributions are for five values of E_T corresponding to 31%-ile, 7%-ile, 4%-ile, 2%-ile, 1/2%-ile .

♡ For a fixed E_T (measured with $\leq 1\%$ resolution), the number of projectile participants varies by $7 - 9\%$ (rms) (depending on the $\delta\eta$) around the mean (μ) at the upper percentiles where 'centrality' is normally defined, increasing to a variation of $\sigma = 10 - 15\%$ about the mean at the lower centrality values (~ 50 projectile participants), with continued proportionality $\sigma/\mu \propto 1/\sqrt{\mu}$ at lower values.

♡ It is hard to imagine that changes of any microscopic physical quantity as a function of measured E_T could be 'sharper' than the variation in Projectile Participants at the same E_T value. Then, of course, measurement resolution further smears the sharpness.

A Weak Point...

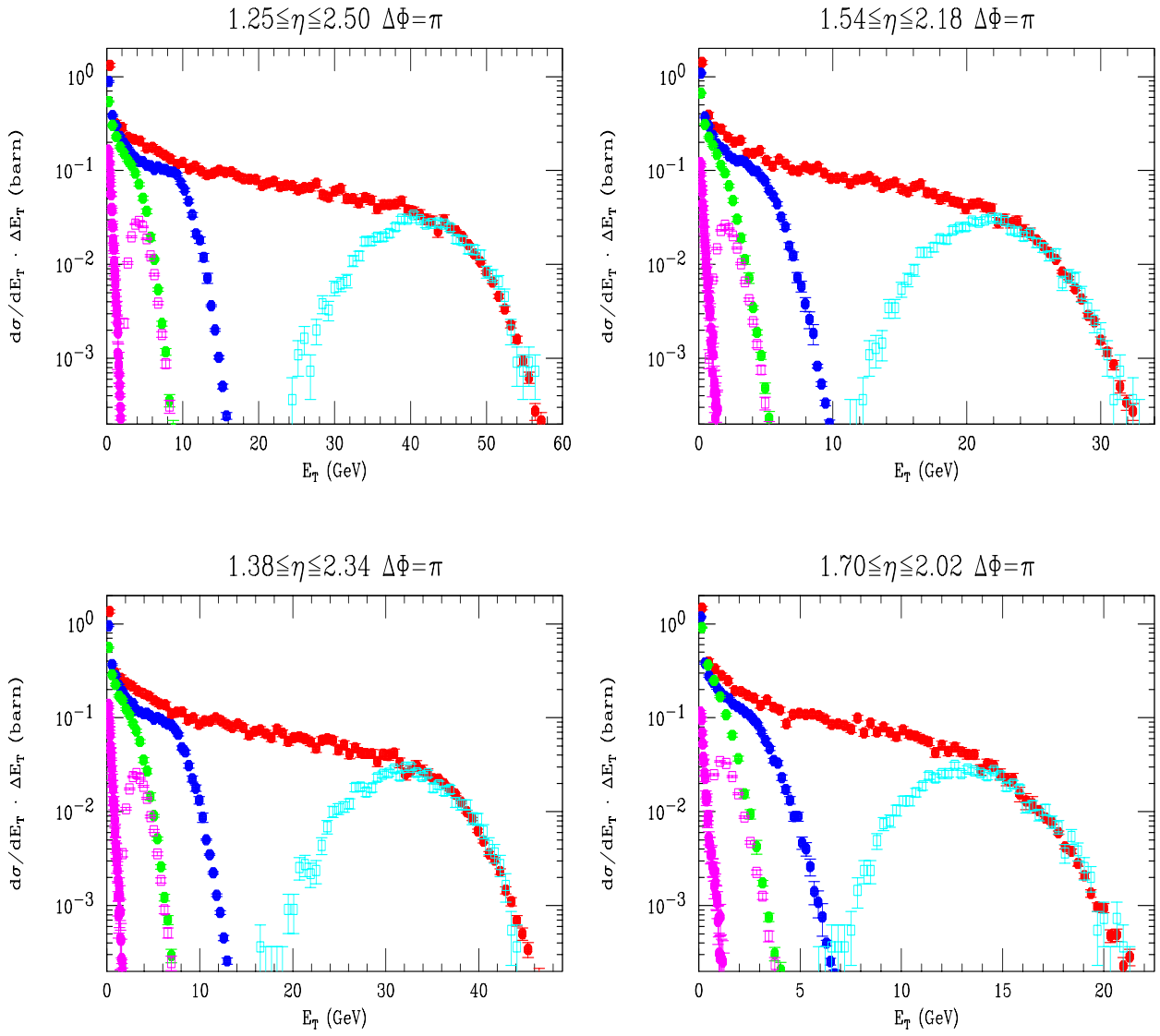

Figure 9: E_T distributions($\Delta\phi = \pi$) for the four $\delta\eta$ intervals indicated, for p+Au, O+Cu, O+Cu (ZCAL), Si+Au, Au+Au, Au+Au (ZCAL). The plotting ranges are chosen by eye to make all the plots look similar.

♡ One problem with the limited aperture, electromagnetic energy event characterization in comparison to '4π' hadron calorimeters is the difficulty in relating the endpoints of the energy spectra—i.e. $\sim$ 32 GeV for $\delta\eta = 0.64$, $\sim$ 22 GeV for $\delta\eta = 0.32$—to the total available energy for the reaction.

Leads to an Improved E_T Plot

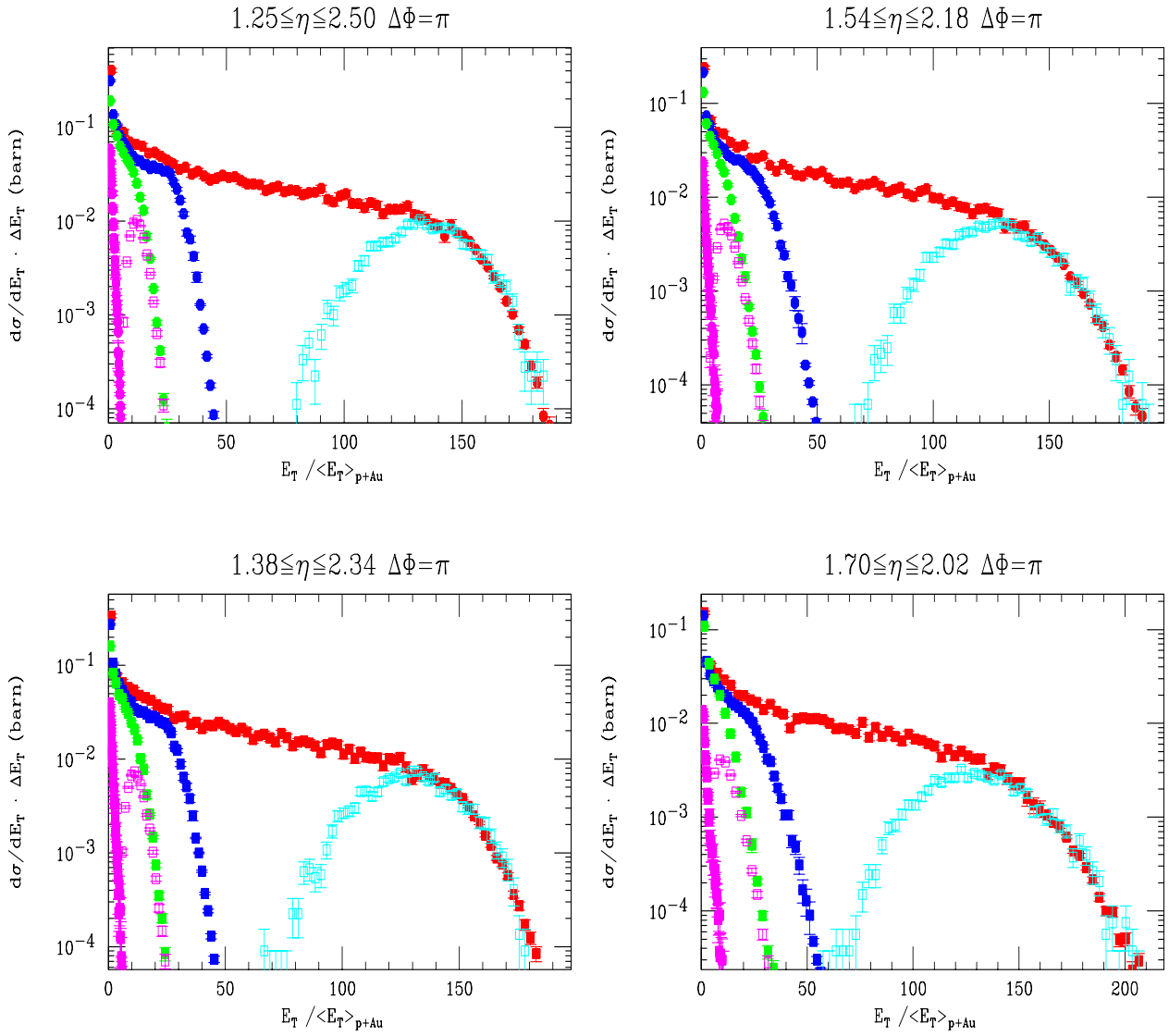

Figure 10: E_T distributions ($\Delta\phi = \pi$) for the four $\delta\eta$ intervals indicated, for p+Au, O+Cu, O+Cu (ZCAL), Si+Au, Au+Au, Au+Au (ZCAL), where the E_T scale is normalized by the measured $\langle E_T \rangle_{\mathrm{p+Au}}$ on the interval. The Au+Au E_T has been scaled up by a factor of 1.155 to correspond to 14.6 GeV/c, see [PL **B332**, 258 (1994)].

♡ When the energy scale for each aperture is plotted in units of the measured $\langle E_T \rangle$ in the same aperture for p+Au collisions (or p-p, if available), the situation changes **dramatically**. The dynamics of the reaction, in terms of projectile (or total) participants, can now be read directly from the figure.

♡ The dynamics of the reaction can now be read directly from the figure.

♡ The p+Au E_T distribution goes out to ~ 7 mean values over 3 orders of magnitude for $\delta\eta = 0.64$, and to ~ 10 mean values over 3 orders of magnitude for $\delta\eta = 0.32$, i.e. the fluctuations around the mean increase with decreasing aperture.

♡ The knees of the O+Cu and Si+Au E_T distributions occur roughly at 16 and 28 times $\langle E_T \rangle_{\mathrm{p+Au}}$ for both apertures, corresponding to the A of the projectiles, but the knee of the Au+Au distribution is roughly 150 and clearly not $A_{\mathrm{Au}} = 197$, apparently indicating some shadowing.

♡ Detailed analysis shows that this is actually an acceptance effect in the limited aperture (ϵ^{197} tends to be considerably less than unity for most reasonable values of ϵ), so that the 'Wounded Projectile Nucleon' actually represents the measurements rather well in all the intervals studied around mid-rapidity at the AGS.

A_p dependence (4%-ile) at Mid-Rapidity for 14.6 A GeV/c

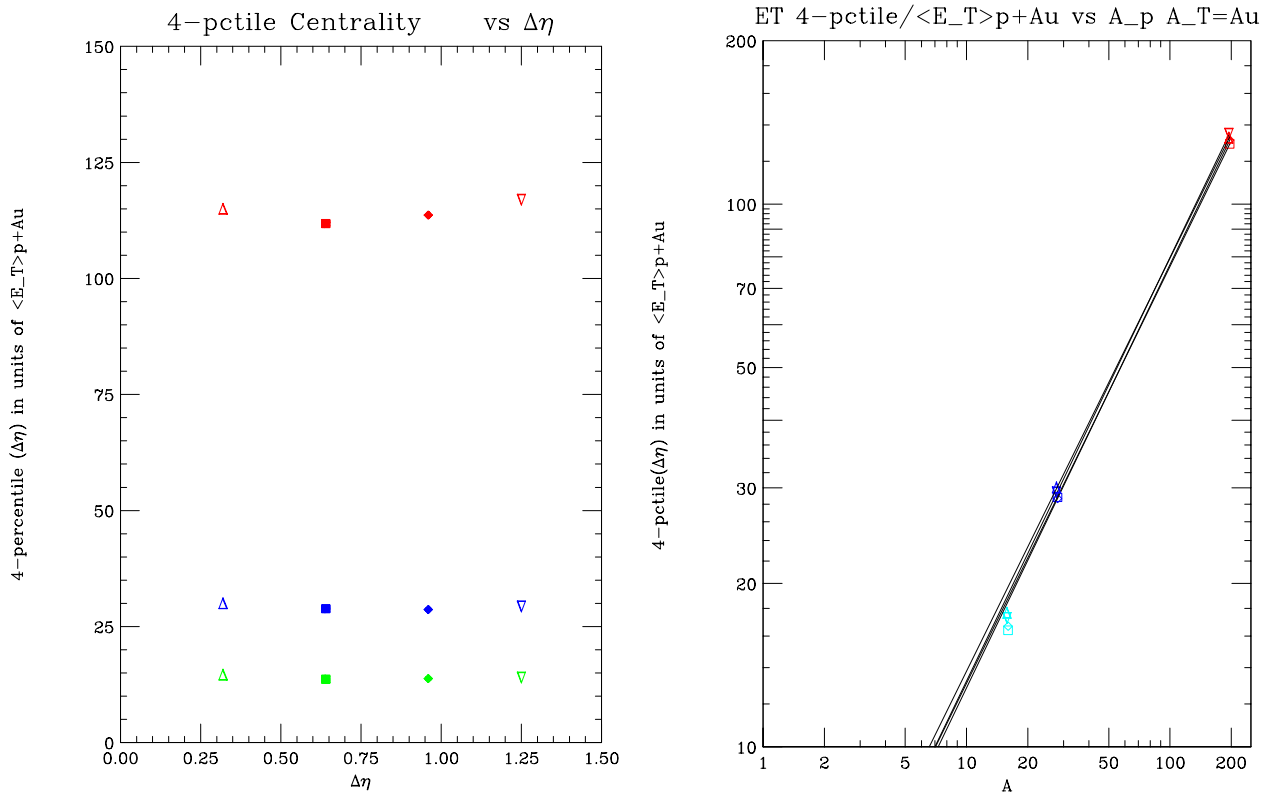

Figure 11: (left) 4%-ile of E_T distributions as a function $\delta\eta$, measured in units of $\langle E_T(\delta\eta)\rangle_{\rm p+A}$: Au+Au (red), Si+Au (blue), O+Cu (green). (right) A_p-dependence of 4%-ile of E_T distributions as a function $\delta\eta$, measured in units of $\langle E_T(\delta\eta)\rangle_{\rm p+Au}$. Lines are fits to $A_p^{\alpha_p}$ from Si+Au to Au+Au (corrected to 14.6 A GeV/c). Cyan points are O+Au from WPNM.

♡ 4%-ile centrality cut is independent of $\delta\eta$, when mesaured in units of $\langle E_T(\delta\eta)\rangle_{\rm p+Au}$.

♡ The same is true for all centralities studied in this work: 7%-ile, 2%-ile, 1%-ile, 0.5%-ile.

♡ With projectile dependence represented as $A_p^{\alpha_p}$: from O+Au to Si+Au, $\alpha_p = 0.94 - 1.00$ depending on %-ile and $\delta\eta$; from Si+Au to Au+Au, $\alpha_p = 0.73 - 0.78$ depending on %-ile and $\delta\eta$.

♡ Stachel at QM'90 showed $A_T^{0.4}$ for S, Si, at both CERN and BNL energies. Any other data for $A_p^{\alpha_p}$??

CONCLUSIONS

- Shapes of E_T distributions change with $\delta\eta$ interval
- The shape $\Gamma(p, b)$ and change of shape with $\delta\eta$ is **Identical** for p+Au and p+Be in E802 for $0.2 \leq \delta\eta \leq 1.25$, around mid-rapidity.
- The shape (or fluctuation) of multiplicity distributions as parameterized by Normalized Factorial Moments or the NBD parameter $1/k = K_2$ can be related to 2-particle correlations by an elegant theoretical framework; but we could find no such framework for the Gamma Distribution parameter $p(\delta\eta)$ nor for E_T correlations.
- The Wounded Projectile Nucleon model works remarkably well to relate all the measured spectral shapes of Electromagnetic E_T distributions from p+Au, to O+Cu, to Si+Au to Au+Au at AGS energies for pseudorapidity intervals $\delta\eta$ in the range $0.2 \leq \delta\eta \leq 1.25$.
- It is clear that E_T distributions in limited regions of $\delta\eta$ provide an excellent characterization of the 'nuclear geometry' of RHI collisions, from which important information about the dynamics can be inferred.
- A new way of plotting E_T distributions was found. If the distribution in any aperture is plotted in units of the measured $\langle E_T \rangle$ in the same aperture for p+Au collisions (or p-p, if available), the dynamics of the reaction, in terms of projectile (or total) participants, can be read directly from the plot.
- At AGS energies, the overall production of particles as observed by mid-rapidity E_T distributions may be interpreted as arising from incoherent nucleon-nucleus collisions, with the further implication that the stopping of the participant nucleons observed in central Au+Au collisions must be related to the identical shapes and evolution of the E_T distributions for p+Au and p+Be. In other words, the 'stopping' should be observable in p+A 'central' collisions.

Systematic measurements of dn/dy and E_T in A+A collisions at the AGS (E802...)

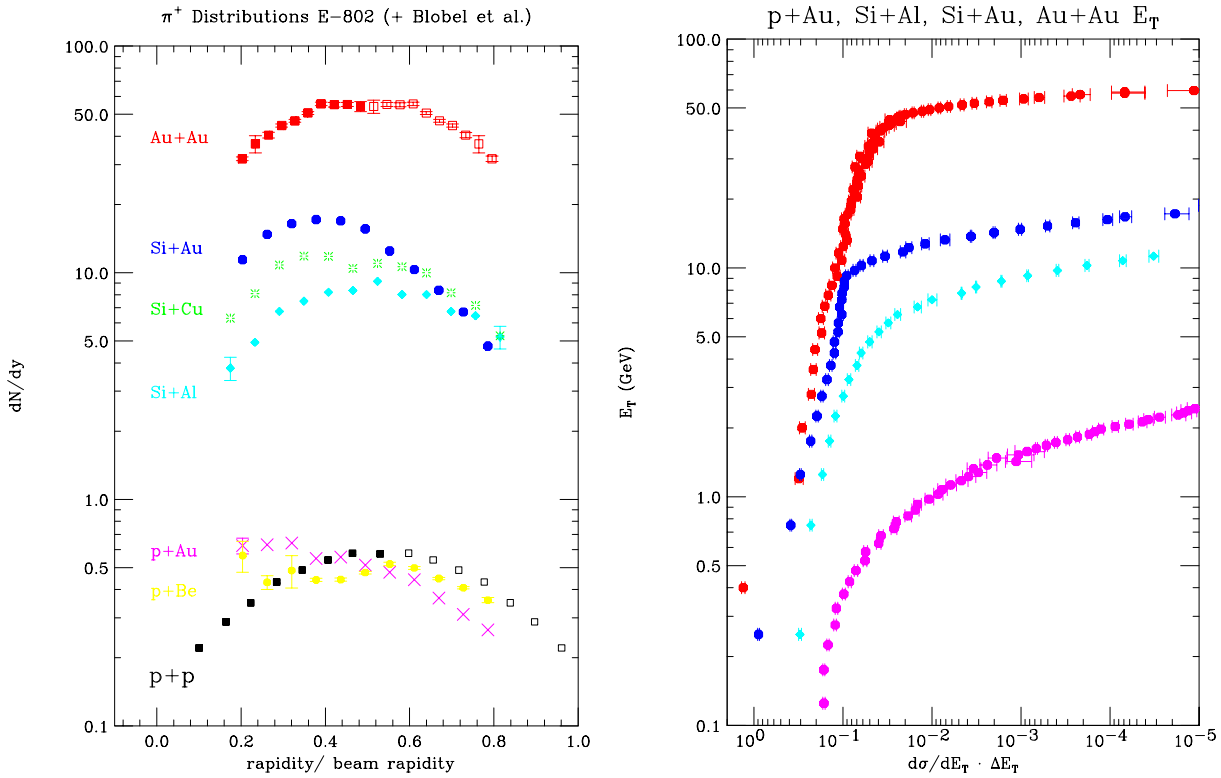

On the left, the $dn/dy|_{\pi^+}$ distributions for p+A inclusive and A+A central track the E_T distributions very well. It easy to see that Au+Au/p-p ∼Au+Au/p+Au=100, much less than 197. Also the p-p or p+Be to p+Au ratios for π^+ evidently don't follow the wounded nucleon model, since dn/dy doesn't vary at mid rapidity, but it does vary in the beam fragmentation region. The comparison Au+Au/Si+Al is intriguing since the Au+Au/Si+Al data for both dn/dy and E_T (right) are close to the WNM ratio of 7. **However,** from the E_T distributions, it is obvious that the exact value of this ratio depends on the "centrality" cut; since the "shapes" of the distributions vary with A and $\delta\eta$. The asymmetric Si+Au,Cu collisions show very interesting systematic behavior c.f. Si+Al, but may be a problem for a mid-rapidity calorimeter since the maximum in dn/dy moves out of the acceptance region. However, as the target dependence of the reaction is clearly emphasized by measurements in the target fragmentation region, while the projectile dependence is emphasized in the projectile fragmentation region, mid-rapidity measurements might represent a reasonable global average.

5 Years of Calibrations

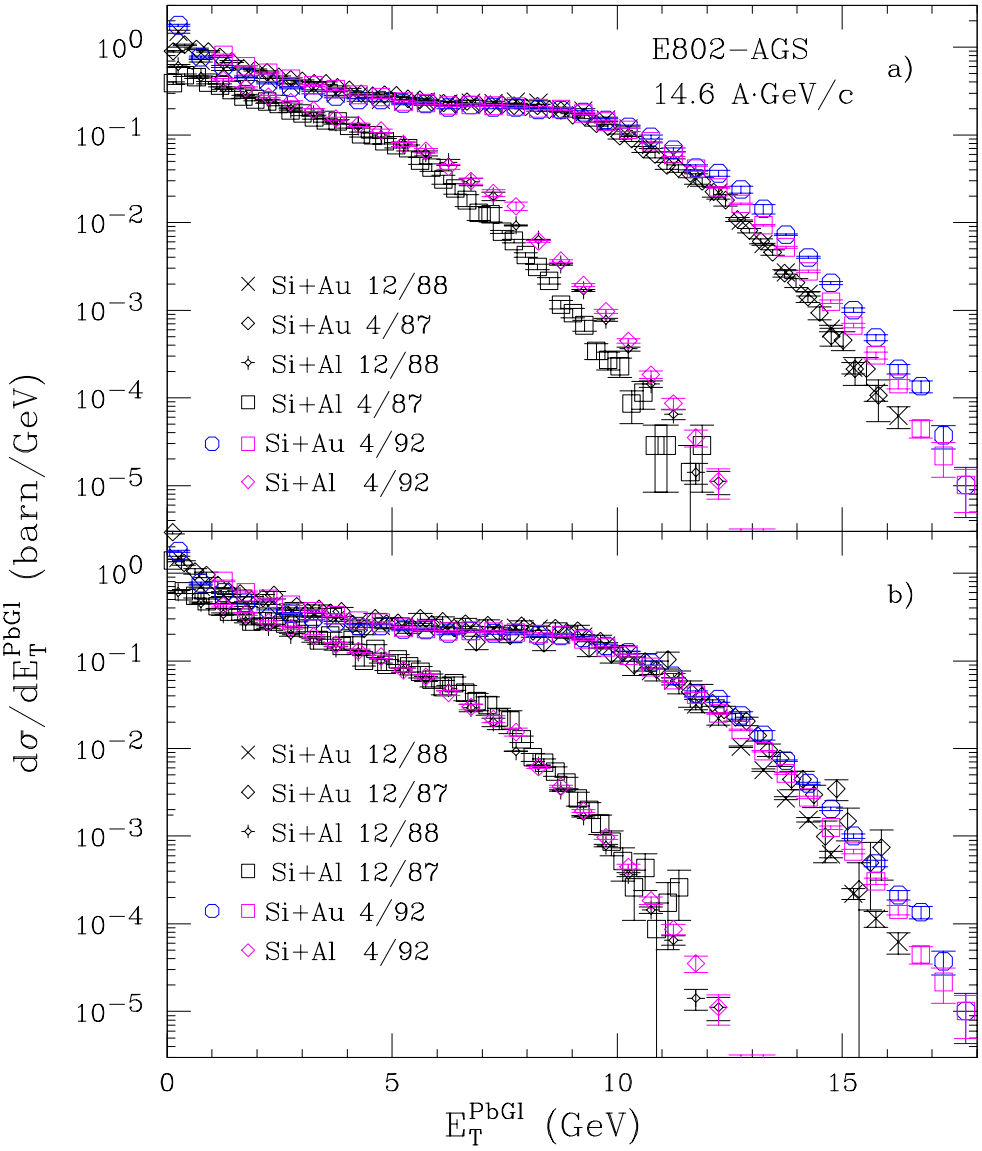

Fig. 11+1992 data

Figure 12: E_T distributions ($\Delta\phi = \pi$, $1.25 \leq \delta\eta \leq 2.50$) for Si+Al and Si+Au from the April 1992 run (which includes Au+Au measurement), compared to measurements in previous runs [PRC **45**, 2933 (1992), Fig. 11].

♡ The 4/92 E_T scale is 3% higher than 12/88, but in excellent agreement with 12/87. ○ and □ are 2 analyses of the same data.

E_T Plots with WPNM fits for all four $\delta\eta$ intervals

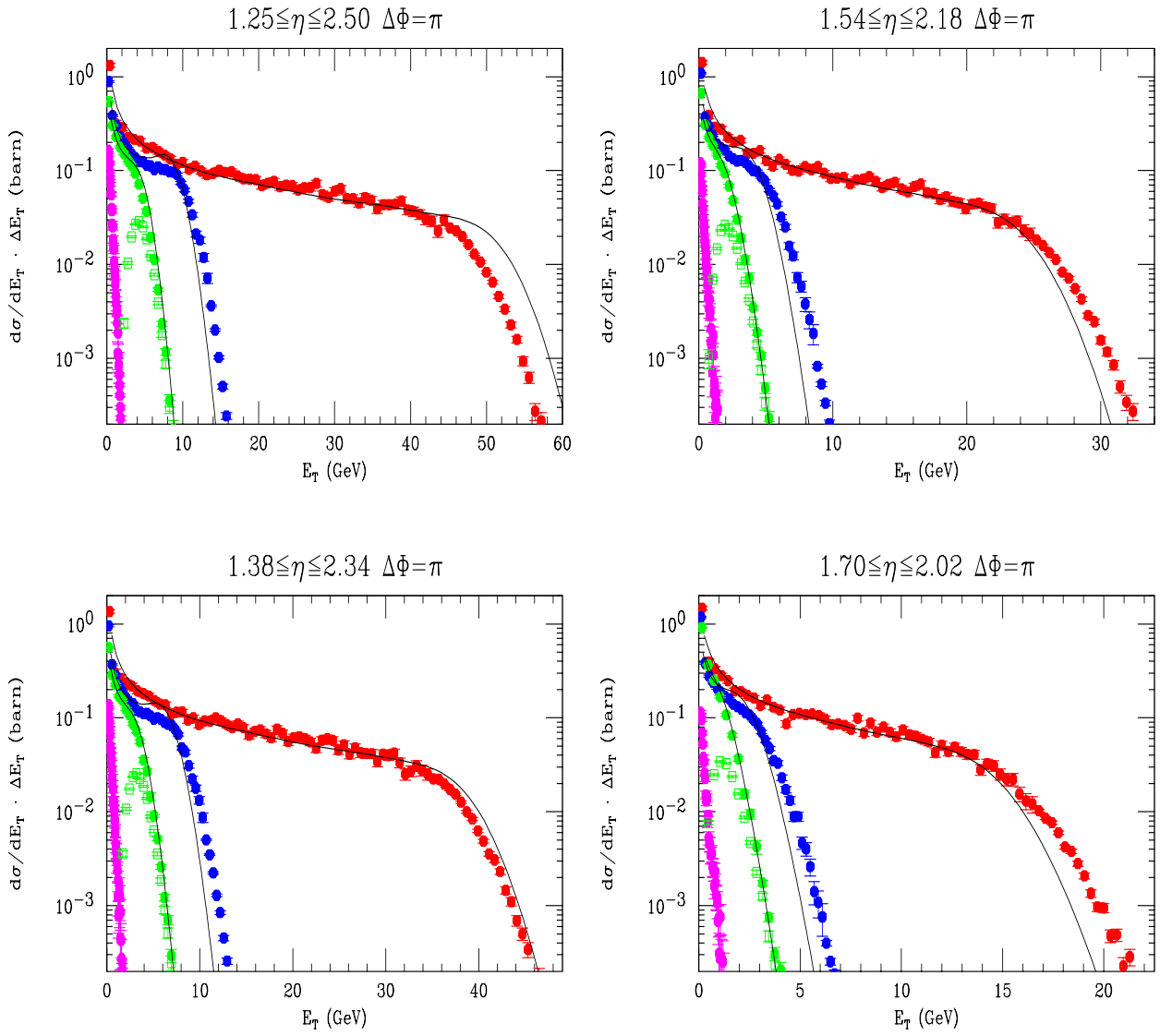

Figure 13: E_T distributions ($\Delta\phi = \pi$) for the four $\delta\eta$ intervals indicated, for p+Au, O+Cu, O+Cu (ZCAL), Si+Au, Au+Au with WPNM calculations (lines) shown. This is Fig. 7 with all intervals shown.

Other Improved E_T Plots

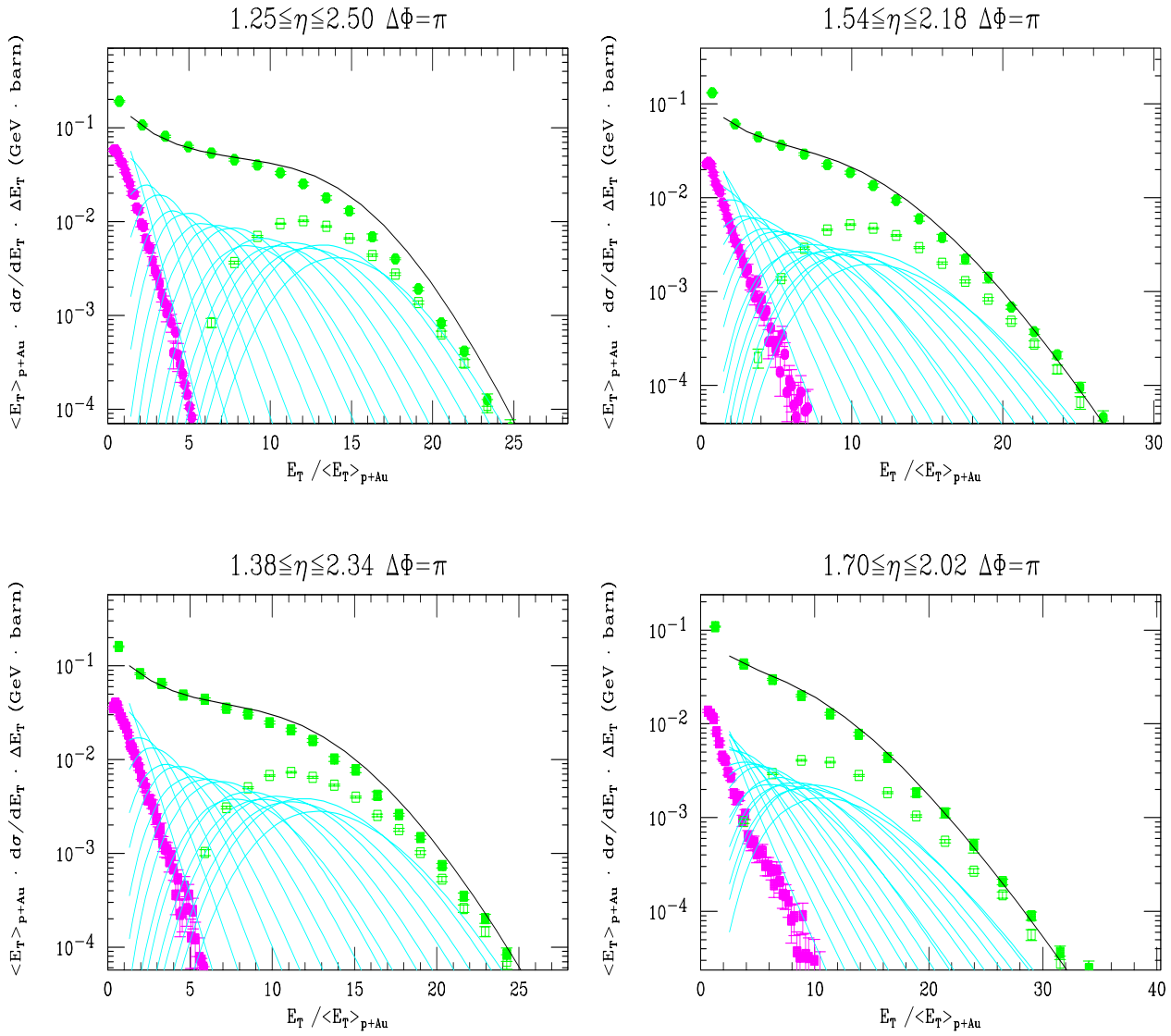

Figure 14: E_T distributions ($\Delta\phi = \pi$) for the four $\delta\eta$ intervals indicated, for p+Au, O+Cu, O+Cu (ZCAL), Si+Au, where the E_T scale is normalized by the measured $\langle E_T \rangle_{\mathrm{p+Au}}$ on the interval.

♡ Also note the 'famous' plot shown on page 7 is plotted in the improved format.

E_T for "Big Buggy" { p,O,Si,Au} + Au, O+Cu

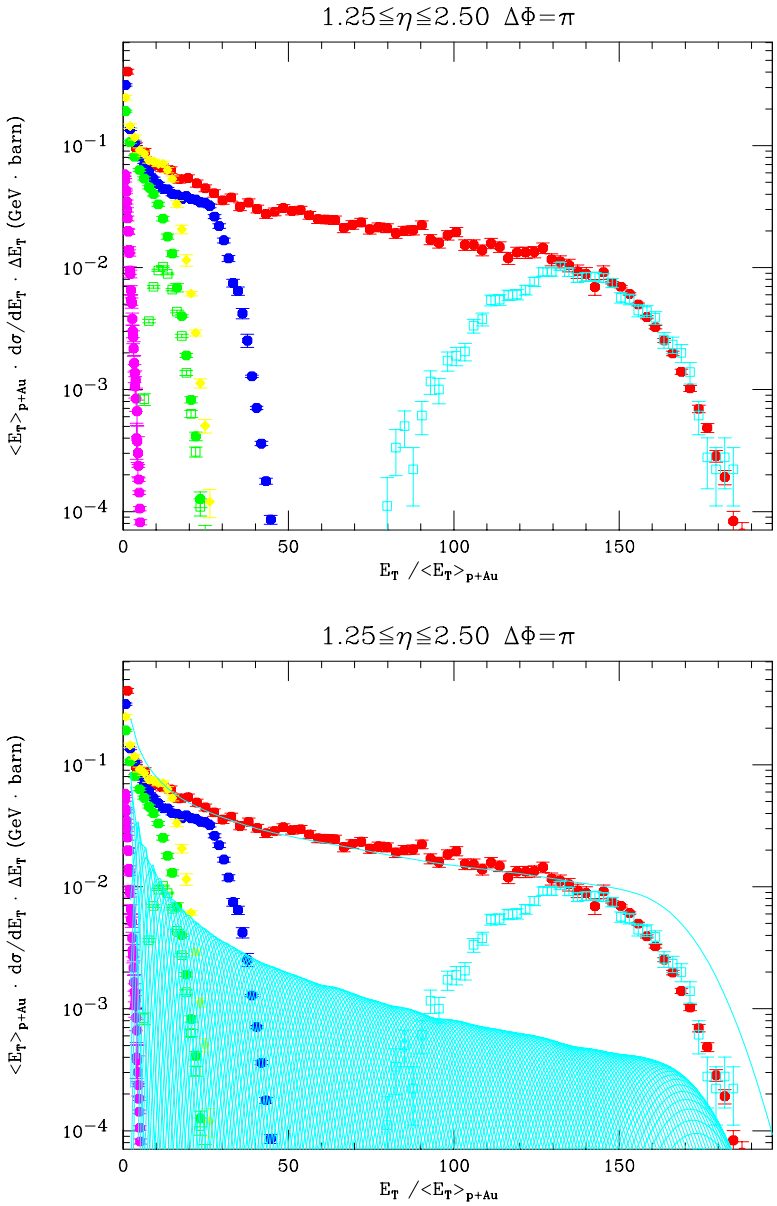

Figure 15: Top(t): E_T distributions ($\Delta\phi = \pi$) in $1.25 \leq \delta\eta \leq 2.50$ for p+Au, O+Cu, O+Cu (ZCAL) , O+Au, Si+Au, Au+Au, Au+Au (ZCAL). Bottom (b) the same with WPNM fit for Au+Au with all components shown

Yes, NA5 Mid-Rapidity E_T Distributions change in shape with $\Delta\Phi$

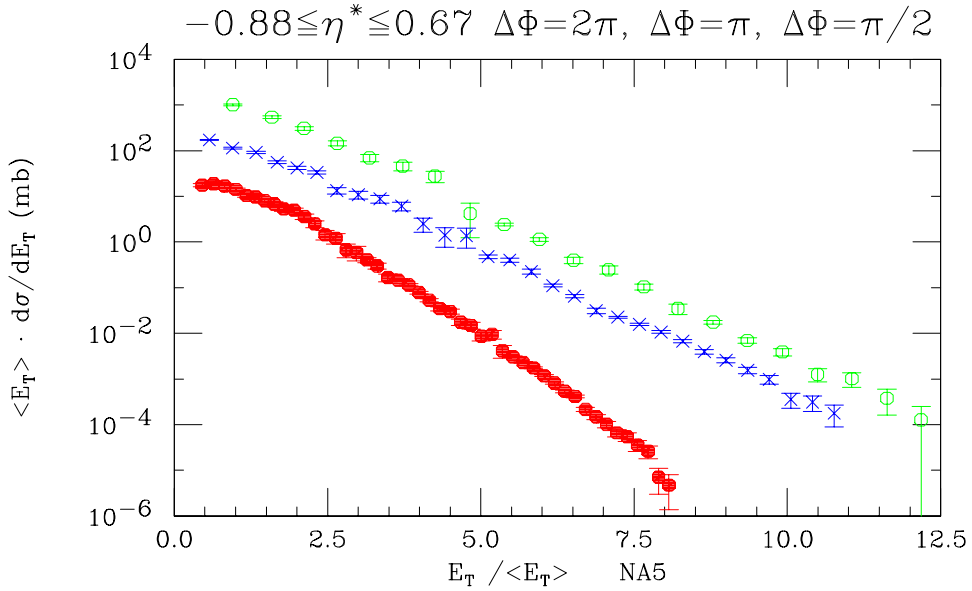

Figure 16: Original NA5 E_T distribution (p-p at 300 GeV) for $\Delta\phi = 2\pi$, π, $\pi/2$ scaled by $\langle E_T \rangle$ in each aperture for $-0.88 \leq \eta^* \leq 0.67$. [PL **112B**, 173 (1982)].

Distributions, Factorial Moments, Cumulants and the Two-Particle Rapidity Correlation

- In short-range rapidity (or pseudo-rapidity) correlation analyses, the normalized two-particle correlation function is usually taken as an exponential:

$$R_2(y_1, y_2) = \frac{\rho_2(y_1, y_2)}{\rho_1(y_1)\rho_1(y_2)} - 1 = R(0,0)\, e^{-|y_1 - y_2|/\xi} \quad , \tag{1}$$

  where $\rho_1(y)$ and $\rho_2(y_1, y_2)$ are the inclusive densities for a single particle (at rapidity y) or 2 particles (at rapidities y_1 and y_2), and ξ is the two-particle short-range rapidity correlation length.

- The two-particle normalized factorial moment (cumulant), F_2 (K_2), is nothing other than the integral of the two-particle correlation function on the interval:

$$K_2(\delta\eta) = F_2(\delta\eta) - 1 = \frac{\int^{\delta\eta} dy_1 dy_2\, \rho_1(y_1)\rho_1(y_2) R_2(y_1, y_2)}{\int^{\delta\eta} dy_1 dy_2\, \rho_1(y_1)\rho_1(y_2)} \quad . \tag{2}$$

- The integrand in the numerator, is the Mueller correlation function, $\mathrm{C}_2(y_1, y_2) = \rho_1(y_1)\rho_1(y_2)R_2(y_1, y_2) = \rho_2(y_1, y_2) - \rho_1(y_1)\rho_1(y_2)$, which is used in the discussion of conventional short-range correlations in multiparticle physics.The denominator of Eq. 2 is simply $<n(\delta\eta)>^2$, the square of the mean multiplicity on the interval.

- For the case of a NBD, $K_2(\delta\eta) = 1/k(\delta\eta)$.

- If the inclusive single particle density, $\rho_1(y) = dn/dy$, is assumed constant on the interval, then the integral can be performed analytically (specifically on the interval $0 \le y_1 \le \delta\eta$, $0 \le y_2 \le \delta\eta$) to obtain the normalized factorial moment $F_2(\delta\eta)$ or normalized factorial cumulant $K_2(\delta\eta)$ in terms of the parameters of Eq. 1:

$$K_2(\delta\eta) = R(0,0)\, G(\delta\eta/\xi) \quad , \tag{3}$$

  where the function $G(x)$ is defined as:

$$G(x) = 2\,\frac{(x - 1 + e^{-x})}{x^2} \quad . \tag{4}$$

Demonstration that the two-pion correlation in rapidity is entirely due to Bose-Einstein correlation